Nano Letters

Supporting Information for "Azimuthal Polarization Filtering for Accurate, Precise, and Robust Single-Molecule Localization Microscopy"

Matthew D. Lew[†,‡] *and W. E. Moerner*[*,†]

[†]Departments of Chemistry and [‡]Electrical Engineering, Stanford University, Stanford, California 94305, United States

*E-mail: wmoerner@stanford.edu

Supporting Figure S1	3D PSFs of azimuthally polarized light from a fixed dipole emitter at various orientations
Supporting Figure S2	Pixelated azimuthally-polarized PSFs and background fluorescence effects on the limit of localization precision
Supporting Figure S3	Simulated fitting of pixelated azimuthally-polarized PSFs and measurement of localization precision
Supporting Note	Mathematical framework for modeling the image formation of single molecules embedded in mismatched media, Details for simulating back focal plane and image plane intensity distributions, and Fisher information matrices for estimation of emitter positions in two dimensions (2D)

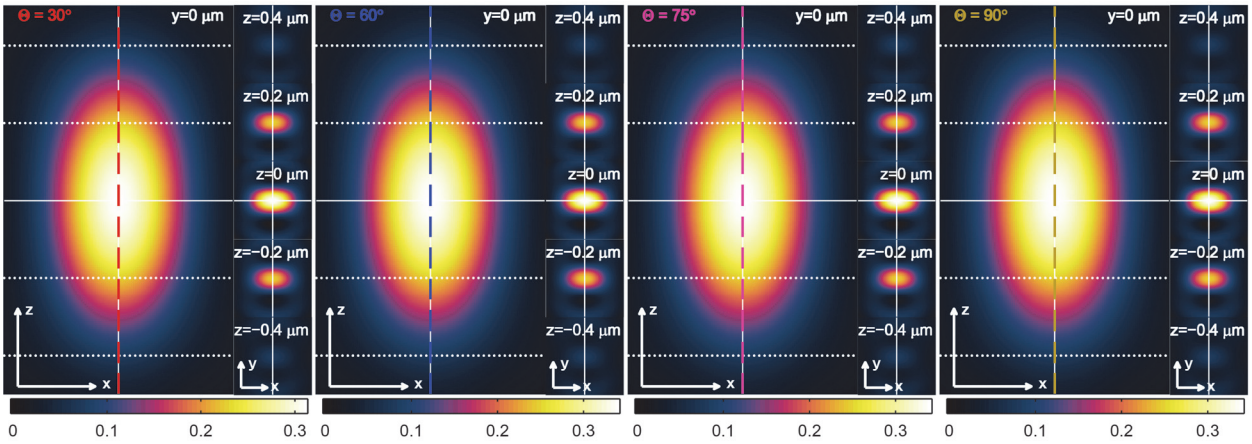

Supporting Figure S1. 3D PSFs of azimuthally polarized light from a fixed dipole emitter at various orientations ($\Phi = 0°$). As a function of polar angle Θ, the images collected by an azimuthally polarized microscope are remarkably similar in shape. Using a 2D elliptical Gaussian function as a model for the PSF results in no localization error regardless of molecular orientation and microscope defocus. The intensity is plotted in units relative to the intensity of a clear-aperture microscope for molecules at identical orientations. Scale axes/arrows = 200 nm.

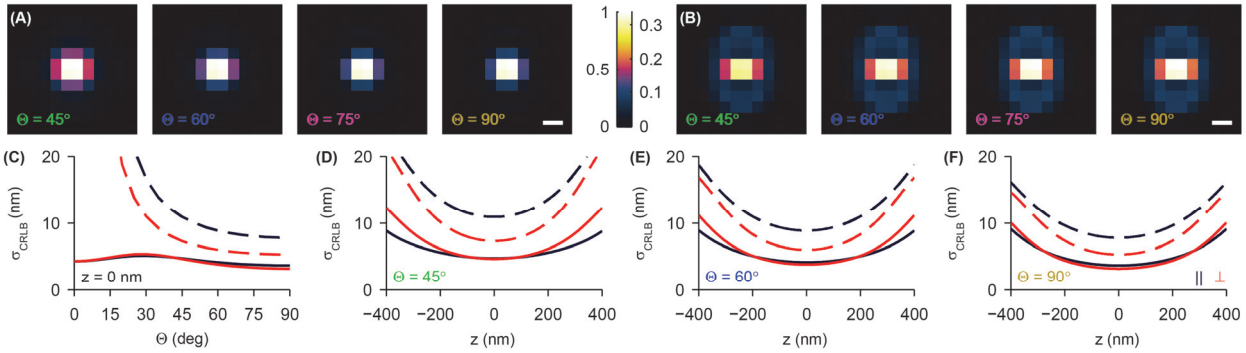

Supporting Figure S2. Pixelated azimuthally-polarized PSFs and background fluorescence effects on the limit of localization precision. (A) Pixelated standard PSF images of an in-focus fixed single-molecule with orientation $\{\Theta = 45°, \Phi = 0°\}$. (B) Same for a microscope with an azimuthal polarization filter. Pixels are 100 nm in size in object space. Scale bar = 200 nm. (C) The 2D limit of localization precision, as computed by the Cramér-Rao lower bound (CRLB), as a function of dipole orientation for the clear aperture microscope (solid lines) and microscope with an azimuthal polarizer (dashed lines) along the direction parallel to the in-plane transition dipole moment ($\mu_x \hat{\mathbf{x}} + \mu_y \hat{\mathbf{y}}$, black lines) and the perpendicular direction (red lines). The effects of 100-nm pixelation and 5 photons/pixel of fluorescence background are included (Equation (S8)). The localization precision of the azimuthal images are 1.7-2.1 times worse than the clear-aperture images for $\Theta = 90°$ (7.8 nm and 5.3 nm in the parallel and perpendicular directions for the azimuthal images, 3.7 nm and 3.2 nm for the unpolarized images). The limit of localization precision is also shown for the same pixelation and background conditions as a function of lens defocus z for (D) $\Theta = 45°$, (E) $\Theta = 60°$, and (F) $\Theta = 90°$. The limit of localization precision for the azimuthally polarized microscope gradually worsens as a function of dipole inclination (8.9 nm and 6.0 nm for $\Theta = 60°$ and 10.9 nm and 7.3 nm for $\Theta = 45°$ in the parallel and perpendicular directions, respectively, at $z = 0$). All calculations assume 1000 photons are captured in the clear aperture microscope images for all molecular orientations and defocus positions, while the azimuthally polarized images have a fewer numbers of detected photons due to a reduced light collection efficiency as shown in Figure 2A.

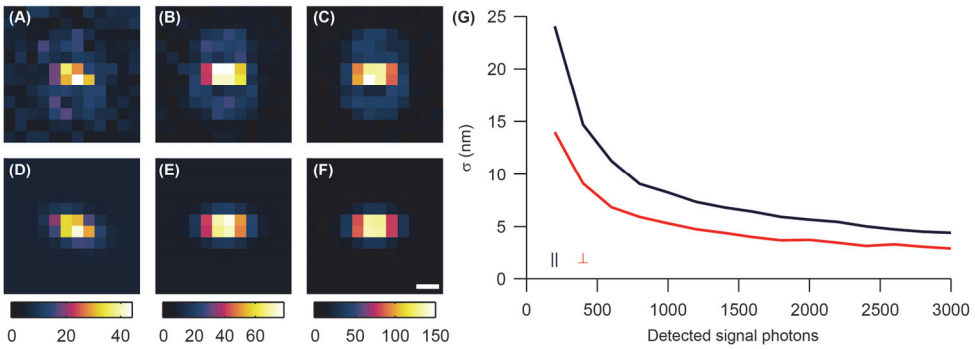

Supporting Figure S3. Simulated fitting of pixelated azimuthally-polarized PSFs and measurement of localization precision. Example realizations of single-molecule images with Poisson shot noise, 100-nm camera pixelation, 5 photons per pixel of background fluorescence, (A) 400 signal photons detected, (B) 1000 signal photons detected, and (C) 2000 signal photons detected. Corresponding 2D elliptical Gaussian fits to these images are shown in (D)-(F). Color scales are in units of total photons per pixel. Scale bar = 200 nm. (G) Localization precision calculated along the direction parallel (black) and perpendicular (red) to the in-plane projection of the transition dipole moment. These precisions are measured from the fitting of a 2D elliptical Gaussian function to 1000 Poisson shot noise realizations of pixelated azimuthally-polarized PSFs with various numbers of detected signal photons. For 600 detected signal photons in the azimuthally-polarized microscope, which corresponds to ~1000 detected signal photons from a single molecule oriented parallel to the coverslip ($\Theta = 90°$) in a clear aperture microscope, the localization precision is 11 nm parallel and 6.8 nm perpendicular to the direction of the in-plane dipole moment. These precisions are 1-4 nm larger than the Cramér-Rao lower bound shown in Supporting Fig. S2(F), demonstrating that least-squares fitting of a 2D elliptical Gaussian function is a computationally efficient and precise way to measure single-molecule positions from an azimuthally-polarized microscope image.

Supporting Note

Mathematical framework for modeling the image formation of single molecules embedded in mismatched media

Here, we modify our expression for the Green's tensor (Equation 5 in the main text) for the presence of an abrupt refractive index change between the immersion media/coverslip and the medium in which the molecule is embedded. This configuration is very common in many forms of optical microscopy, especially in the case of imaging biological specimens, when using an objective lens with large numerical aperture (typically requiring immersion oil $n_1 = 1.518$) to image single molecules in aqueous media ($n_2 = 1.333$). If the molecule emits light from above the interface, the various rays will be refracted by that interface, leading to spherical aberration.[1, 2] Furthermore, if the molecule is close to the interface (its depth $z_d < \lambda$) and $n_2 < n_1$, then the evanescent field emitted by the molecule can couple into propagating waves through the objective lens.

The modified Green's tensor $\mathbf{G}_{bfp}^{\rho\phi z}\left(\rho,\phi,z_d\right)$ is given by[3]

$$\mathbf{G}_{bfp}^{\rho\phi z}\left(\rho,\phi,z_d\right)=\frac{\exp\left(in_1kf_{obj}\right)}{4\pi f_{obj}}\sqrt{\frac{n_1}{n_0\left(1-\rho^2\right)^{1/2}}}\begin{bmatrix} c_2\cos\left(\phi\right)\sqrt{1-\rho^2} & c_2\sin\left(\phi\right)\sqrt{1-\rho^2} & -c_1\rho \\ -c_3\sin\left(\phi\right) & c_3\cos\left(\phi\right) & 0 \\ 0 & 0 & 0 \end{bmatrix}, \quad \text{(S1)}$$

where the constants $\left\{c_1,c_2,c_3\right\}$ are defined as

$$\begin{aligned} c_1 &= \left(\frac{n_1}{n_2}\right)^2\frac{\cos\left(\theta_1\right)}{\cos\left(\theta_2\right)}t^p\left(\theta\right)\exp\left[ikz_dn_2\sqrt{1-\left(n_1/n_2\right)\rho^2}\right] \\ c_2 &= \left(\frac{n_1}{n_2}\right)t^p\left(\theta\right)\exp\left[ikz_dn_2\sqrt{1-\left(n_1/n_2\right)\rho^2}\right] \\ c_3 &= \left(\frac{n_1}{n_2}\right)\frac{\cos\left(\theta_1\right)}{\cos\left(\theta_2\right)}t^s\left(\theta\right)\exp\left[ikz_dn_2\sqrt{1-\left(n_1/n_2\right)\rho^2}\right] \end{aligned} \quad . \quad \text{(S2)}$$

The angles θ_1 and θ_2 are the polar inclination of rays propagating from the objective lens to the sample. They are related to the radial coordinate ρ in the back focal plane by

$$\theta_1 = \sin^{-1}\left(\rho\right)$$
$$\theta_2 = \sin^{-1}\left(\rho\frac{n_1}{n_2}\right) . \quad \text{(S3)}$$

Finally, $t^p\left(\theta\right)$ and $t^s\left(\theta\right)$ are the Fresnel transmission coefficients for P- and S-polarized light, respectively, propagating from the objective lens into the sample. These equations can be plugged directly into Equation 6 (main text) to compute the electric field in the back focal plane or Equations 8-10 (main text) to compute the image of the single molecule.

Details for simulating back focal plane and image plane intensity distributions

Images of the back focal plane of a standard microscope are calculated by evaluating the field intensity $\left\|\mathbf{E}_{bfp}^{xyz}\right\|^2$ from the definition of the Green's tensor given by

$$\mathbf{E}_{bfp}^{xyz}\left(\rho,\phi,z\right)=A\exp\left[in_1kz\left(1-\rho^2\right)^{1/2}\right]\mathbf{G}_{bfp}^{xyz}\left(\rho,\phi\right)\hat{\boldsymbol{\mu}}, \tag{S4}$$

where definitions of these quantities are given in the main text. To create a back focal plane image of an azimuthally polarized microscope, an additional tensor $\mathbf{P}^{\rho\phi z}$ representing an azimuthal polarizer is inserted into the above expression, yielding

$$\mathbf{E}_{bfp}^{xyz}\left(\rho,\phi,z\right)=A\exp\left[in_1kz\left(1-\rho^2\right)^{1/2}\right]\mathbf{R}^{-1}\left(\phi\right)\mathbf{P}^{\rho\phi z}\mathbf{R}\left(\phi\right)\mathbf{G}_{bfp}^{xyz}\left(\rho,\phi\right)\hat{\boldsymbol{\mu}}, \tag{S5}$$

where the spatially-varying rotation matrix $\mathbf{R}\left(\phi\right)$ is utilized to convert between Cartesian and cylindrical bases and

$$\mathbf{P}^{\rho\phi z}=\begin{bmatrix}0&0&0\\0&1&0\\0&0&0\end{bmatrix}. \tag{S6}$$

To simulate 3D PSFs of the standard microscope, $\left\|\mathbf{E}_{img}^{xyz}\right\|^2$ is evaluated using equations (10) in the main text and (S4) above for various amounts of defocus z. Similarly, 3D PSFs of an azimuthally polarized microscope can be evaluated using equations (10), (S5), and (S6).

Fisher information matrices for estimation of emitter positions in two dimensions (2D)

The analytical expression for the Fisher information matrix for 2D localization is given by

$$\mathbf{I}(\xi) = \operatorname{diag}\left[\begin{array}{l} \iint_{\mathbb{R}_2} \frac{1}{q(x,y,z)}\left(\frac{\partial q(x,y,z)}{\partial x}\right)^2 \mathrm{d}x\,\mathrm{d}y \\ \iint_{\mathbb{R}_2} \frac{1}{q(x,y,z)}\left(\frac{\partial q(x,y,z)}{\partial y}\right)^2 \mathrm{d}x\,\mathrm{d}y \end{array}\right], \tag{S7}$$

where $q(x,y,z)$ is the 2D PSF image of an emitter located at position $\{x,y,z\}$ scaled by the expected number of photons captured by the imaging system such that $\iint_{\mathbb{R}_2} q(x,y,z)\,\mathrm{d}x\,\mathrm{d}y = N$ and ξ represents the 2D position of the emitter. Note that the Fisher information increases with the square of the gradient of the PSF; sharper, more confined PSFs lead to better localization precision. This expression models the Poisson shot noise associated with the detection of photons by a camera but neglects the effects of pixelation, detector read noise or excess noise, and fluorescence background.

Incorporating pixelation and fluorescence background effects into the Fisher information matrix is relatively straightforward. Converting the continuous integral over an infinite detector into a discrete sum over a finite number of pixels and adding an offset to the signal,[4, 5] the modified expression is given by

$$\mathbf{I}(\xi) = \operatorname{diag}\left[\begin{array}{l} \sum_{k=1}^{N_p} \frac{1}{\mu_{xyz}[k] + \beta[k]}\left(\frac{\partial \mu_{xyz}[k]}{\partial x}\right)^2 \\ \sum_{k=1}^{N_p} \frac{1}{\mu_{xyz}[k] + \beta[k]}\left(\frac{\partial \mu_{xyz}[k]}{\partial y}\right)^2 \end{array}\right] \tag{S8}$$

where N_p is the number of detector pixels sampling the PSF, $\mu_{xyz}[k]$ is the mean number of signal photons detected by the kth pixel from a molecule at position $\{x,y,z\}$ relative to the focal plane, and $\beta[k]$ is the mean number of background photons detected by the kth pixel.

References

1. Hell, S. W.; Reiner, G.; Cremer, C.; Stelzer, E. H. K. *J. Microsc.* **1993***, 169,* 391-14.

2. Wiersma, S. H.; Torok, P.; Visser, T. D.; Varga, P. *J. Opt. Soc. Am. A* **1997***, 14,* 1482-1490.

3. Backer, A. S.; Moerner, W. E. *J. Phys. Chem. B* **2014***, 118,* 8313-8329.

4. Ober, R. J.; Ram, S.; Ward, E. S. *Biophys. J.* **2004***, 86,* 1185-1200.

5. Ram, S.; Prabhat, P.; Chao, J.; Ward, E. S.; Ober, R. J. *Biophys. J.* **2008***, 95,* 6025-6043.